

Two-photon absorption in liquid xenon

C. A. Whitehead, H. Pournasr, and J. W. Keto

Physics Department, The University of Texas at Austin, Austin, Texas 78712

(Received 5 August 1992; revised manuscript received 19 October 1992)

Excitation spectra of two-photon excited xenon near the triple point have been obtained in order to study exciton structure near the band edge. While the band gap is suppressed in the low-temperature liquid, absorption due to even-parity exciton states is presented and discussed. The even-parity $\Gamma_{3/2, n=2}$ Wannier excitons observed in the liquid are shifted approximately 0.12 eV to higher energies relative to the energy of odd-parity excitons observed in the liquid by Beaglehole. The absorption linewidths (full width at half maximum) are measured to be 0.15 eV. Comparisons are made to one-photon absorption spectra in xenon.

I. INTRODUCTION

Although one-photon absorption has been studied previously in condensed xenon,¹⁻⁴ we present here the results of two-photon excitation scans through the band edge of liquid xenon during which direct excitation of the even-parity exciton levels is observed. Justification for measurements of the excitonic structure of condensed rare gases lies mainly in the close correspondence between the fluorescence of the trapped exciton in the liquid and the excimer in the gas. Exciton self-trapping rates and fluorescence efficiencies in liquid and solid xenon have been measured with an eye towards utilization of such as a lasing medium.

While similar measurements have been performed on alkali halides,^{5,6} these data are a direct observation of even-parity excitons in condensed xenon. The one-photon excitation scans of Beaglehole² and Subtil *et al.*⁷ in liquid xenon yield linewidths consistent with those of the data reported here, but, while the $2s$, odd-parity excitons observed in those experiments are shifted by approximately 0.03 eV to the red^{2,7,8} relative to the $2s$ exciton in the solid at 160 K, the even-parity bands excited by two-photon absorption in the liquid are shifted approximately 0.085 eV towards the blue. We present a model estimating the shift between the $2s$ and $2p$ excitons due to central cell corrections which is consistent with the measured shift of 0.115 eV. Further investigation of excitons in solid xenon is warranted to present an all-inclusive model.

II. EXPERIMENT

Xenon gas was allowed to enter a stainless steel sample cell from a high-purity stainless steel gas handling system. The cell and gas handling system were baked at 400°C for three or four days until an ultimate pressure of 10^{-9} Torr was achieved. The xenon gas (99.9995% pure from Spectra-Gas, Inc.) was purified further over a titanium sponge held at 900°C. After entering the sample chamber, the gas was condensed to a liquid by boiling off liquid nitrogen at 77 K and flowing the vapor through $\frac{1}{8}$ -inch copper tubing silver-soldered around the outside of

the sample cell. The temperature was regulated using a Lakeshore Cryogenics Model DRC 80C to within 0.1 K with a Lakeshore Model DT-500 silicon diode supplying the temperature feedback. Current was supplied to a nichrome wire wrapped around the body of the sample cell to adjust the temperature to within the desired range. Due to the large difference in coefficients of expansion between stainless steel and solid xenon at 160 K, efforts to lower the temperature of the sample below the triple point resulted in fracturing of the crystal at the interface of the stainless wall and the cryocrystal. The fissures produced by this tearing away from the walls rapidly spread throughout the crystal until it became opaque to the laser beam. This fracturing occurred within 1° of the triple point thus prohibiting studies of the solid.

Following laser excitation, vuv fluorescence passed through a MgF₂ window mounted on top of the cell and was analyzed using a modified Seya 1-meter monochromator to which was attached an EMR Model 541N-09-13-03900 phototube. An attempt was made to detect visible or infrared (IR) fluorescence using a 1-meter Jobin-Yvon monochromator with an RCA 8852 phototube but fluorescence from two-photon excited liquid xenon was not observed in this wavelength region. Laser light passed into the sample cell through sapphire windows sealed onto flanges on either end by gold O-rings. See Fig. 1 for experimental setup. Radiation tunable between 245–300 nm was generated by frequency doubling the output of a Hansch-type dye laser pumped by a Spectra-Physics DCR-2 pulsed Nd:YAG (yttrium aluminum garnet) laser. Three dyes (Coumarin 500, Coumarin 540, and Rhodamine 610) were pumped by the tripled output of the YAG to cover the range of excitation of the exciton states and band edge. Frequency doubling was achieved with a beta-barium borate (BBO) crystal to obtain 0.5 mJ of horizontally polarized uv radiation which was focused in the center of the cell to a spot size of $\sim 15 \mu\text{m}$. Pulse widths were 6 nsec and the laser bandwidth at the doubled wavelength was approximately 0.4 cm^{-1} ($5 \times 10^{-5} \text{ eV}$). The uv beam was first sent through an uncoated quartz flat whose front surface reflection was directed onto an EG&G FND-100 absolutely calibrated photodiode to obtain the laser energy on a pulse-to-pulse

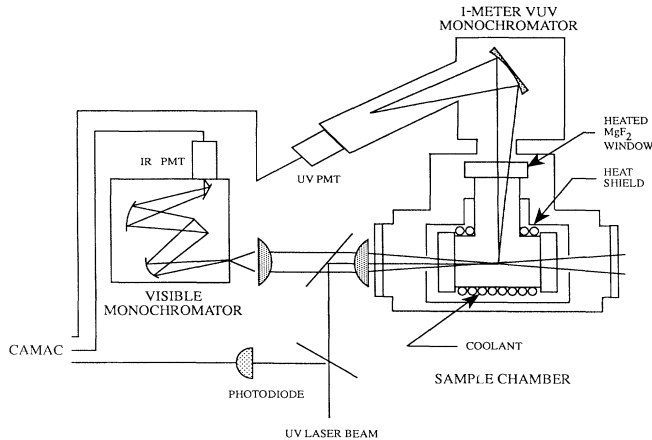


FIG. 1. Experimental apparatus for two-photon excitation scans of liquid xenon.

basis. Fluorescence measurements following laser excitation were normalized to the square of this energy measurement in order to remove the variations in laser energy over the large tuning range and the pulse-to-pulse fluctuations in laser energy.

III. RESULTS AND DISCUSSION

After absorption of two quanta of energy from the focused laser, an exciton consisting of an electron and hole bound one to the other are created. This exciton is free to move throughout the crystal; however, Roick, Gaethke, and Zimmerer³ have shown that the rate of trapping of these excitons in solid xenon to form quasi-molecular centers is rapid and limited in the high-temperature limit by the Debye frequency of the lattice. Assuming that the lattice structure of the liquid remains essentially unchanged during the pulse width of the laser, we extrapolate to obtain a self-trapping rate of $\sim 8 \times 10^{12} \text{ sec}^{-1}$. After creation, these excitons are trapped immediately into a local lattice deformation whose fluorescence is similar to that of the excimer in the dense gas at 1730 Å but is Stokes shifted by roughly 30 Å. By monitoring this quasimolecular fluorescence and scanning the laser as a function of energy, we obtain the two-photon excitation scan shown in Fig. 2. The step size of the frequency-doubled light for this scan was 0.01 eV and 500 laser shots were taken at each spectral point. Indicated in the figure are the positions of the $\Gamma(\frac{3}{2})n=1,2,3$ excitons in solid xenon at 160 K as determined by Subtil *et al.*;⁷ also indicated is the band edge observed in the solid. The small bands at 8.8, 9.55, and 9.75 eV have been reproduced in subsequent scans but are currently unassigned. Due to the difficulties inherent in producing short-wavelength tunable radiation, no attempt was made to scan through the $\Gamma(\frac{1}{2})n=2,3,\dots$ exciton bands although suggestions for future work would include such a scan.

We have fitted the two features between 9.0 and 9.5 eV with a Gaussian line shape using a nonlinear least-squares fit. The best fit is shown as the solid line in Fig. 2 and the mean energies and widths are reported in Table I.

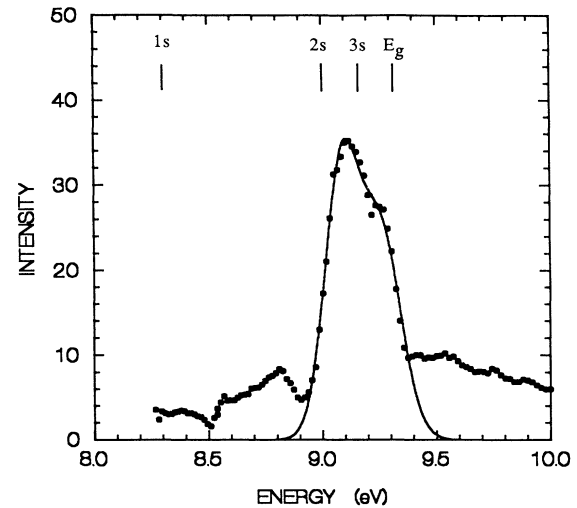


FIG. 2. Two-photon excitation spectra of liquid xenon at 162 K. Indicated are the positions of the 1s, 2s, and 3s excitons in solid xenon at 160 K as measured by Subtil, *et al.*, Ref. 7. Also shown is the band gap for the solid at 160 K. The intensity is in arbitrary units.

Figure 3 shows a fluorescence scan following excitation at 9.2 eV. At each spectral point, 200 laser shots were taken. Since no filters were used on the vuv monochromator, the strong feature near 2500 Å is laser scattered light. The strongest fluorescence feature is the self-trapped exciton luminescence at 1750 Å. The weak band at 3600 Å is unidentified but has been observed in the dense gas excited by electron bombardment. Fluorescence scans were attempted in the region 5000–10 000 Å, but no luminescence attributable to relaxation in the liquid was observed.

At the Γ point in the Brillouin zone of the xenon lattice, the valence band is comprised of atomic *p* orbitals of the ground-state atom while the lowest conduction band is made up of *s* orbitals of the first excited states. Direct two-photon transitions from the valence to lowest conduction band are therefore not allowed. This explains the absence of a band edge in the excitation scan. The conduction band at the *X* point of the Brillouin zone, which is thought to comprise mainly *p* orbitals, has a band gap of approximately 12 eV (Ref. 9) and would be another good argument for scans to shorter wavelengths. Two-photon excitation scans in the alkali halides exhibit no excitonic structure, while the band edge is readily apparent. Frohlich and Stagninus⁵ suggest two possibilities

TABLE I. Liquid xenon, $T=162 \text{ K}$. Reported errors are 2σ .

State	Energy (eV)	Full width at half maximum (eV)	References
1s $\Gamma(\frac{3}{2})$	8.145	0.3	2,7,13
2s $\Gamma(\frac{3}{2})$	8.97	0.15±0.01	7,12
2p $\Gamma(\frac{3}{2})$	9.085±0.022	0.149±0.011	This work
3p $\Gamma(\frac{3}{2})$	9.257±0.034	0.172±0.022	This work

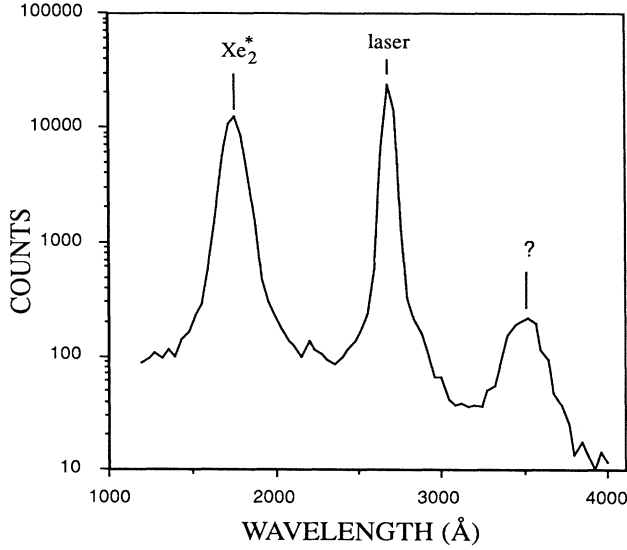


FIG. 3. Fluorescence scan following excitation of liquid xenon at 9.2 eV.

for the appearance of the band edge in alkali halides under two-photon absorption: (1) forbidden transitions at the Γ point, and (2) allowed transitions to bands of different symmetry. Neither of these models accounts for the absence of the band edge in xenon. A more detailed study of the symmetry of the valence and conduction bands would have to be undertaken to explain this disparity.

A. Rydberg Model for Excitons

Models for excitons in condensed rare gases have been recently reviewed.^{10,11} The Wannier model has been shown to accurately model the energies for s -exciton in the rare gases for $n \geq 2$.

$$E_{n,j} = E_{\infty,j} - B_j / n^2. \quad (1)$$

Here the exciton is modeled as an electron bound by the Coulomb attraction to the valence hole with either $j = \frac{1}{2}$ or $j = \frac{3}{2}$ at the center of the Brillouin zone [often referred to as $\Gamma(\frac{1}{2})$ and $\Gamma(\frac{3}{2})$ excitons]. E_{∞} is the Rydberg convergence limit and B_j is the exciton binding energy,

$$B = \mu R / \epsilon^2, \quad (2)$$

where $\mu = m_e m_h / (m_e + m_h)$, m_e and m_h are the effective masses of the electron and hole, R is the Rydberg, and ϵ is the relative dielectric constant for the solid or liquid. For the $2p$ and $3p$ excitons listed in Table I, $B = 1.24 \pm 0.3$ eV and $E_{\infty} = 9.39 \pm 0.29$ eV. Using $\epsilon = 1.94$, as measured by Sinnock for liquid xenon near the triple point,¹² we estimate the reduced effective mass for the exciton, $\mu = 0.34 \pm 0.08$. These values compare to $E_{\infty} = 9.30$ eV and $\mu = 0.36$ for the solid near the triple point.^{7,13}

In liquid xenon, Reshotko *et al.*¹³ estimated the effective mass of the $2s$ exciton over a range of densities. Since the $3s$ exciton is not observed in liquid xenon,^{1,7,11}

they estimated the binding energy from the Rydberg series limit which they determined from measured threshold values E_{th} for photoconductivity.¹⁴ In solid xenon at the triple point, E_{∞} exceeds the threshold value, $E_{th} = 9.265$ eV, by 0.38 eV; presumably because of thermal ionization of photoexcited excitons near the conduction band.¹³ Assuming that the same difference $E_{\infty} - E_{th}$ applies to the liquid at the same temperature, Reshotko *et al.* estimated $E_{\infty} = 9.22$ eV and $\mu = 0.27$ for liquid xenon at the triple point. We find the $2p$ and $3p$ excitons observed by two-photon excitation to be closer to the solid than to the liquid, when comparing these simple Wannier models.

The blue shift between the $2p$ and $2s$ exciton observed in the liquid and compared in Table II suggests a breakdown of the Wannier model, since the energies of the hydrogenic model described by Eq. (1) are independent of l . Such a shift is common in alkali atoms because of decreased screening of the ion core caused by greater penetration of the s orbital compared to the p orbital. In the alkali atoms the screening is accurately accounted for by a quantum-defect model of the Rydberg series,

$$E_n = E_{\infty} - R / (n' - \delta_l)^2, \quad (3)$$

where n' is the principal quantum number for the valence electron. For excitons it is common to assume a quantum-defect model

$$E_n = E_{\infty} - B / (n + \delta)^2, \quad (4)$$

where $n = 1, 2$, etc. and n already takes into account screening in the ion core (hole).

There has been recent debate about the efficacy of a quantum-defect model in describing excitons in the condensed rare gases.^{15,16} In an earlier paper,¹⁷ Resca and Resta used the quantum defect to provide a Rydberg picture of the exciton series which accurately included the $n = 1$ resonance. This model assumed the electron-hole interaction to be that of the isolated atom for an electron radius inside of the atomic radius. Outside of the atomic radius the Wannier effective-mass model for the exciton was used. The solutions were then logarithmically matched at the atom radius. Resca and Resta found calculated quantum defects which agreed reasonably with fits of Eq. (4) to the data. With more precise measurements of the band gap in neon,¹⁸ Bersnstorff and Saile found that a least-squares fit using a constant quantum

TABLE II. Central cell correction for the $n = 1$ and $n = 2$ excitons for liquid xenon at the triple point. Energies are in atomic units, μ/ϵ Hartrees. Hermanson, Ref. 20 obtained $\Delta E = -0.025$ a.u. for the solid. For Eqs. (6.8) of Ref. 20, we used the parameters $a = (0.86)^{-1}$ a.u., $Q = 0.5$ (a.u.)⁻¹, and the atom radius, $r_0 = 4.2$ a.u. For solid xenon, $\epsilon = 2.23$, $\mu^* = 0.31$, while for liquid xenon, $\epsilon = 1.94$, $\mu^* = 0.34$.

	V_R	V_{DB}	V_{KE}	ΔE (liquid)	ΔE (solid)
1s	+0.361	-0.0155	-0.276	+0.069	-0.021
2s	+0.043	-0.0014	-0.090	-0.048	
2p	+0.001	-0.0004	-0.023	-0.022	

defect to include the $n=1$ exciton yields $E_\infty = 21.61 \pm 0.08$ eV compared to a band gap $E_G = 21.48_{-0.08}^{+0.04}$ eV, while a simple Wannier fit for all excitons $n > 1$ gave better agreement. The groups don't disagree on the applicability of the quantum-defect model in principle, but disagree on the exact nature of the potential applicable within the central cell. Saile *et al.* argue that Resca and Resta's atomic potential inside of R ignores known changes in both the dielectric constant and effective mass within the atomic radius that adequately accounts for the energy shift of the $1s$ exciton, and that the exciton states for $n \geq 2$ might be best described in the simple Wannier picture. This picture requires a quantum defect for *only* the $1s$ exciton.

In atomic systems, the screened effective charge Ze seen by the valence electron falls rapidly with increasing radius decreasing to $Z=1$ at $r=r_0$. For the region $r < r_0$ [on the order of 1 bohr (0.53 Å) for xenon] where $Z(r) > 1$, the kinetic-energy term dominates the solution of Schroedinger's equation,¹⁹ giving nearly the same radial wave function (within a normalization factor) for $r < r_0$ for all n (given the same l). For the region $r > r_0$, the potential is Coulombic with a hydrogenic solution shifted to $n' = n - \delta_l$ in order to match the interior wave function at r_0 . As the eigenenergy increases, n' increases by 1, giving nearly the same quantum defect for all n .

These effects would also apply to the interaction of the electron with the hole in the exciton. Indeed the higher energy observed for the $2p$ exciton compared to the $2s$ exciton might naively be attributed to lesser penetration into screened charge of the multielectron hole; but for excitons, the problem is considerably more complicated than atomic effects. Just outside of r_0 (on the order of one atomic unit, 0.53 Å, for xenon), the potential seen by the electron is Coulombic, $V = -e/r$, but by two atomic units the potential converges to $-e/\epsilon r$ due to the dielectric screening of the solid.²⁰ This change in dielectric constant has been modeled by Hermanson.²⁰ In reducing the potential, the dielectric screening spreads the electron wave function to larger r , which in turn decreases the expected quantum defect. Because of the large dielectric constant for xenon, one expects that for $n \geq 2$ the quantum defects are small and that the Wannier model is approximately correct. Additional effects in the solid such as polarization of the hole and the change in the effective mass for radii inside of the central cell further complicate a calculation. The effective mass converges from the atomic value at small r to the effective mass over a range of 5 Å.²⁰ In the region outside of r_0 and inside of the central cell, over which the effective mass changes, the kinetic energy will not dominate the solution of Shroedinger's equation and the wave function and this *additional* quantum defect may not be independent of n . In contrast to the above picture, the Wannier model assumes that the effect of both the dielectric and effective mass continues to $r=0$; Resca and Resta's model assumes that the dielectric and effective mass change stepwise to their solid values at the atom radius.

We have attempted a quantum-defect model for the $1s$, $2s$, $2p$, and $3p$ exciton states of liquid xenon. At the value $E_\infty = 9.22$ eV estimated by Reshotko *et al.*¹³ we would

obtain unreasonable values as the measured $3p$ energy (9.26 eV) lies above E_∞ . Given the experimental errors in determining the exciton energies, we cannot condemn this convergence limit; but it is physically reasonable that E_∞ lies higher in energy. As discussed previously, Reshotko *et al.* assumed that $E_\infty - E_{th}$ is due to thermal activation and has the same values as for the solid at the same temperature. The exciton widths in the liquid however, are considerably broader than for the solid, hence excitons further from the band edge may be thermally ionized, leading to photoconductivity thresholds E_{th} which are further from the band edge in liquids than in solids. For lack of a better alternative we assume $E_\infty = 9.3$ eV, the value for the solid at the triple point. In general for solid xenon, the constant quantum-defect model for the $1s$, $2s$, and $3s$ excitons results in $E_\infty = E_G$. Using $E_\infty = 9.3$ eV and the energies for the $1s$ and $2s$ excitons from Table I, we calculate the parameters: $\delta_s = -0.104$ and $B = 0.928$. Using the energy of the $2p$ exciton from Table I, we calculate $\delta_p = +0.077$. These three parameters yield an energy for the $3p$ exciton of 9.202 eV. This is on the low side of the energy extracted in Table I, but within the experimental error. With the addition of the energy measurement of the $3p$ exciton (9.257 eV) and again assuming $E_\infty = 9.3$ eV, we attempted a simultaneous solution of the Rydberg equations using the measured value for the $3p$ exciton and independent quantum defects for δ_{1s} and δ_{2s} in order to account for the expected central cell corrections. Since the radius for $1s$ exciton is well within the central cell, while the radii for $n \geq 2$ is well outside, such a change with n is only expected for $n=1$. The binding energy determined by this model is too different from the solid, and the quantum defects are too large. Larger values for the binding energy and smaller values for the quantum defects can be obtained for larger values of E_∞ .

B. Central Cell Corrections

Because of dielectric screening, the radius for an $n=2$ exciton is approximately three times the nearest-neighbor distance. This greatly decreases the amplitude for the wave function within the ion core, and greatly decreases the expected quantum defect for these states. Resca and Resta found, for their model of solid xenon, the quantum defects were "negligible" for all n and they state that the Rydberg and Wannier formulas agree with the experimental data for the same values of E_∞ and B .²¹ With these arguments one might reasonably assume that the expected shifts for the $n=2$ excitons would be significantly smaller and that the $2s$ and $2p$ states should be degenerate. This is in disagreement with the experimental results.

Because of this discrepancy between an intuitive understanding and the experimental, we have estimated the central cell corrections for the $2s$ and $2p$ excitons in liquid xenon using the results of Hermanson.²⁰ In his calculations, he considered three contributions: (1) an effective local repulsive potential V_R [Eq. (6.8c) of Ref. 20], (2) a perturbation of the Wannier model due to the change in dielectric constant within the central cell V_{DB}

[Eq. (6.8a) of Ref. 20], and (3) a perturbation due to the nonparabolic nature of the energy bands V_{KE} [Eq. (6.8b) of Ref. 20]. Since we find the latter is the most significant for the $n=2$ excitons, we reproduce it here (with the removal of a typographic minus sign):

$$V_{KE} = \frac{\hbar^2}{2m} \left(\frac{m}{\mu^*} - 1 \right) \times \left[\frac{\exp(-r/a)\nabla^2 + \nabla^2 \exp(-r/a)}{2} \right], \quad (5)$$

where a is a radial cutoff parameter for the change in effective mass,

$$m/\mu(r) = m/\mu^* - (m/\mu^* - 1) \exp(-r/a). \quad (6)$$

Before making a pseudopotential calculation for the $n=1$ exciton, Hermanson first estimated the shift using perturbation theory. Since we expect that the perturbation approach is reasonably accurate for the $n=2$ excitons, we have used a similar model by numerically integrating the perturbations of Eq. (6.8) of Ref. 20 for the $n=1$ and $n=2$ exciton states for liquid xenon. We used hydrogen atom wave functions expected from the Wannier picture as the first-order solution.²² In Table II we compare our results for the total-energy shift for solid xenon using the equations and parameters of Hermanson's paper, and we obtain results consistent with Hermanson's results of Table IV of Ref. 20; energies are listed in atomic units, rather than the fractional shift relative to the energy of the $1s$ exciton used by Hermanson. For the liquid calculations, we used the reduced exciton mass $\mu^*=0.34$ and dielectric constant $\epsilon=1.94$. Note that the electrostatic perturbations V_R and V_{DB} are small for the $n=2$ excitons as expected, but the perturbation due to Eq. (5) is significant. Table II predicts that the $2p$ exciton lies

higher in energy than the $2s$ exciton by 0.064 eV compared with the experimental difference of 0.115 ± 0.029 eV observed in Table I. This is reasonable agreement considering the lack of an accurate estimate for μ^* in liquid xenon and expected deficiencies in Eq. (5).²⁰ More exact calculations require detailed models for the conduction bands in solid xenon similar to the calculations of Rössler.²³

IV. CONCLUSION

Though a more precise value of the effective mass for the exciton is needed for a definite conclusion, the Wannier model with central cell corrections appears to reasonably predict the shift in energy between the $2s$ and $2p$ excitons of the liquid. This model for liquid xenon is limited by the large widths and small number of resonances observed in the liquid which results in an uncertainty in both E_∞ and the exciton mass; a more accurate picture may be possible for the solid. While data for even-parity excitons in the solid are needed to fully understand the exciton structure, an initial observation of even-parity excitons in condensed rare gases has been achieved. Future work will concentrate on obtaining two-photon absorption data on the solid at low temperatures to avoid the broadening caused by phonons present at higher temperatures. We also plan to extend the region of excitation to shorter wavelengths.

The authors would like to express their gratitude to Professor Gianni Ascarelli and Professor George Zimmerer for many enlightening ideas and discussions during the course of this experiment. This research was supported by the US DOE, Division of Chemical Sciences, Office of Basic Energy Sciences, and the Robert A. Welch foundation. The authors also would like to acknowledge financial support from NATO.

¹G. Baldini, *Phys. Rev.* **128**, 1562 (1962).

²D. Beaglehole, *Phys. Rev. Lett.* **15**, 553 (1965).

³E. Roick, R. Gaethke, and G. Zimmerer, *Solid State Commun.* **47**, 333 (1983).

⁴P. Laporte, N. Damany, and J.-L. Subtil, in *Photophysics and Photochemistry above 6 eV*, edited by F. Lahmani (Elsevier, Amsterdam, 1985).

⁵D. Frohlich and B. Stagninus, *Phys. Rev. Lett.* **19**, 496 (1967).

⁶J. J. Hopfield, J. M. Worlock, and K. Park, *Phys. Rev. Lett.* **11**, 414 (1963).

⁷J. L. Subtil, P. Laporte, R. Reininger, and V. Saile, *Phys. Status Solidi B* **143**, 783 (1987).

⁸B. SonnTag, in *Rare Gas Solids*, edited by M. L. Klein and J. A. Venables (Academic, London, 1977) Vol. II, p. 1049.

⁹U. Rössler, *Phys. Status Solidi* **42**, 345 (1970).

¹⁰G. Zimmerer, *Excited-State Spectroscopy in Solids*, XCVI Corso (Soc. Italiana di Fisica, Bologna, Italy, 1987).

¹¹Irene Ya. Fugol, *Adv. Phys.* **27**, 1 (1977).

¹²A. C. Sinnock, *J. Phys. C*, **13**, 2375 (1980).

¹³M. Reshotko, U. Asaf, G. Ascarelli, R. Reininger, G. Reinfeld, and I. T. Steinberger, *Phys. Rev. B* **43**, 14 174 (1991).

¹⁴R. Reininger, U. Asaf, I. T. Steinberger, V. Saile, and P. La-

porte, *Phys. Rev. B* **28**, 3193 (1983).

¹⁵V. Saile, R. Reininger, P. Laporte, I. T. Steinberger, and G. L. Findley, *Phys. Rev. B* **37**, 10 901 (1988).

¹⁶Lorenzo Resca, *Phys. Rev. B* **37**, 10 898 (1988).

¹⁷L. Resca and R. Resta, *Phys. Rev. B* **19**, 1683 (1979).

¹⁸S. Bersnstorff and V. Saile, *Opt. Commun.* **58**, 181 (1986).

¹⁹John C. Slater, *Quantum Theory of Atomic Structure* (McGraw-Hill, New York, 1960), Vol. I, pp. 229-232.

²⁰J. Hermanson, *Phys. Rev.* **150**, 660 (1966).

²¹L. Resca and R. Resta, *Phys. Rev. B* **19**, 1683 (1979). In determining a "negligible" quantum defect the authors must disregard the observed experimental shift of the $1s$ exciton from the Wannier Series, $\Delta E=0.042$ eV, as discussed by Hermanson in Ref. 20 and Rössler, p. 533 of Ref. 23. We have fitted the exciton resonances as listed in Ref. 10 above and obtain a quantum defect $\delta=+0.09$. While this quantum defect is small, it is not "negligible."

²²We used the radical equations $R_{1s}=2 \exp(-r)$, $R_{2s}=2^{1/2}(1-r/2) \exp(-r/2)$, and $R_{2p}=24^{-1/2}r \exp(-r/2)$.

²³U. Rössler, in *Rare Gas Solids*, edited by M. L. Klein and J. A. Venables, (Academic, London, 1976), Vol. I, pp. 503-557.